



# The $S_{pb}$ method used to estimate crack extension for coiled tubings fracture toughness tests



J. Wainstein <sup>a,\*</sup>, J.E. Perez Ipiña <sup>b</sup>

<sup>a</sup> UNPSJB-UNPA-CIT Golfo San Jorge-CONICET, Ruta Prov. 1 km 4, Comodoro Rivadavia 9000, Chubut, Argentina

<sup>b</sup> GMF-LPM, UNComa-CONICET, Buenos Aires 1400, Neuquén 8300, Argentina

## ARTICLE INFO

### Article history:

Received 27 December 2016

Received in revised form 10 March 2017

Accepted 11 March 2017

Available online 14 March 2017

### Keywords:

$S_{pb}$  method

Coiled tubings

Separability property

Crack growth estimation

## ABSTRACT

Coiled tubings are widely used in oil and gas industries. Fracture toughness test of coiled tubing is a challenge. Non-standard specimen has to be used due to its geometrical difficulties, ie small thickness and diameter. Taking into account these factors, fracture toughness resistance curves,  $J$ - $R$  curves, of coiled tubings were determined using the  $S_{pb}$  method for the first time. The separability parameter,  $S_{pb}$ , is defined as the load ratio between two specimens at constant displacement, a precracked one that exhibits crack growth during its test and a blunt notched specimen with constant crack length when tested.  $S_{pb}$  method, which uses  $S_{pb}$  parameter, estimates stable crack growth in fracture toughness tests. It has been applied to different standardized specimen geometries. In this work, the method is applied to non-standard coiled tubing specimens. The geometry function was experimentally obtained testing four-point bending specimens. Stable crack growth results are compared to those measured using DC potential drop method used as reference method. Encouraging results were obtained.

© 2017 Elsevier Ltd. All rights reserved.

## 1. Introduction

*Coiled Tubing* are thin walled steel tubes of 25–89 mm in diameter and several thousand meters long. They are used in oil and energy industries to provide a number of production tasks and maintenance services. They suffer plastic deformation during unwinding of the reel, passing through a *goose neck* arch guide and an injection unit. Strain levels are about 2–3%, making the tubing fails by low cycle fatigue in around 100 wrap-unwrap cycles. The fracture behavior of a component is necessary to know in order to assess the integrity of structures containing crack like defects. For pipe materials with high toughness, elastic-plastic fracture mechanics (EPFM) provides realistic estimates of the fracture performance of cracked pressurized pipes. *Coiled tubing* made of high strength low alloy (HSLA) steel behaves in a ductile manner at working temperatures in and out the well. Under operational conditions, a circumferential crack generally initiates at the inner surface of the tube. Then the crack can grow through the thickness. Two possibilities may arise in this situation:

- (a) Sudden rupture may take place before the crack reaches the surface, causing a break before leak condition. In this case, the crack growing through the thickness, reaches its critical crack size. It must be taken into account that the critical crack size could be changing in every tensile strain cycle [1].

\* Corresponding author.

E-mail address: [jwainste@gmail.com](mailto:jwainste@gmail.com) (J. Wainstein).

**Nomenclature**

$a$	crack length
$a_p$	precracked crack length
$a_b$	blunt notched crack length
$b$	remaining ligament
$b_0$	blunt notched initial remaining ligament
$b_b$	blunt notched remaining ligament
$C$	half crack arc length
$2C$	crack arc length
$2C_0$	initial crack arc length
$2C_f$	final crack arc length
$C(T)$	compact tension specimen
$CC(T)$	center cracked panel tension
$D$	coiled tubing external diameter
$D1i$	measure of initial roundness, vertical direction
$D1f$	measure of final roundness, vertical direction
$D2i$	measure of initial roundness, horizontal direction
$D2f$	measure of final roundness, horizontal direction
$G$	geometry function
$H$	deformation function
$J$	$J$ integral
$J_{IC}$	$J$ value at crack growth initiation
$m$	exponent $S_{pb}$ method equation
$P$	applied load
$P_p$	precracked applied load
$P_b$	blunt notched applied load
$S$	span
$SE(B)$	single edge notched bend specimen
$SE(T)$	single edge notched tension specimen
$S_{ij}$	separability parameter blunt notched specimens of $i$ and $j$ crack length
$S_{pb}$	separability parameter of a precracked and a blunt notched specimen
$t$	thickness
$W$	coiled tubing perimeter used as width
$\gamma$	a function to correct $J$ integral in crack growth situations
$\eta_{pl}$	etha plastic factor, a function to multiply the area under $P$ - $v$ curve to get $J$ integral
$v$	displacement
$v_{pl}$	plastic component of displacement

(b) The crack can grow through the thickness until it reaches the outer surface and attains a leak before break condition. It becomes a through wall thickness crack. In case the tube is not repaired or taken out of service, subcritical crack growth may occur after this condition, until a critical crack size is reached, and the total failure occurs.

Although both cases (a) and (b) can occur in service operation, according to the experience related by users, case (b) takes place in most operation conditions. At the outside and inside well temperatures, the tube material works in the upper shelf in which the failure mode can be by ductile tearing. In this situation, the material  $R$  curve is necessary to make an instability analysis.

Fracture toughness of ductile materials is often characterized by the  $J$ -integral concept proposed by Rice [2]. The determination of characteristic values is generally performed through the construction of the material resistance curve ( $J$ - $R$  curve). Stable crack growth has to be estimated for this purpose and different alternatives are available. The first method used was the multiple specimen technique developed by Begley and Landes [3] in which several identical specimens are loaded to obtain different amounts of crack growth. The crack lengths are then physically measured on the fracture surfaces after the specimens have been broken. This method is not always a practical one because large amounts of material and time are required for specimen preparation and testing. For this reason, considerable efforts were devoted to develop methods consuming less time and material [4–7]. The most common single specimen testing methodologies applied in the field of metals are the elastic-unloading compliance and the electrical potential drop techniques. They require special equipment for on-line measurement of crack extension, are more difficult to implement and present limitations when applied to some materials or conditions [8,9].

$S_{pb}$  method, was developed [10,11] and successfully applied to fracture toughness of metals and polymers characterization [12–16], including high load rate conditions [17]. This concept was originally proposed for several other related appli-

cations: to determine the  $\eta_{pl}$  factor in pre-cracked specimens, to set up the limits of validity in load separation and to determine the stable crack growth initiation parameter,  $J_{IC}$ , without the need of building the  $J$ - $R$  curve [8,18,19].

The  $S_{pb}$  method, as normalization, is based on the existence of the load separation proposed by Ernst et al. [20]

$$P = G\left(\frac{a}{W}\right) \times H\left(\frac{v_{pl}}{W}\right) \tag{1}$$

where  $G(a/W)$  is the geometry function and  $H(v_{pl}/W)$  is the deformation properties function.

The  $S_{pb}$  parameter is defined as the load ratio between two specimens at constant displacement, a precracked one that exhibits crack growth during its test and a blunt notched specimen with constant crack length when tested.

$$S_{pb} = \frac{P_p(a_p, v_{pl})}{P_b(a_b, v_{pl})} \Big|_{v_{pl}} = \frac{G_p\left(\frac{a_p}{W}\right) \cdot H\left(\frac{v_{pl}}{W}\right)}{G_b\left(\frac{a_b}{W}\right) \cdot H\left(\frac{v_{pl}}{W}\right)} \Big|_{v_{pl}} \tag{2}$$

Sharobeam and Landes [21] studied the load separability property in several precracked specimen geometries (C(T), SE (B), CC(T) and SE(T)), as well as in different materials. For situations when the geometry function,  $G(a/W)$ , can be fitted by a potential function

$$G\left(\frac{a}{W}\right) = \left(\frac{a}{W}\right)^m \tag{3}$$

They proved that the  $S_{pb}$  parameter adopts the following expression:

$$S_{pb} = \frac{P_p}{P_b} \Big|_{v_{pl}} = \left(\frac{a_p}{a_b}\right)^m \tag{4}$$

$$a_p = a_b(S_{pb})^{1/m} \tag{5}$$

The  $S_{pb}$  method is a simple technique for crack length estimation usually applied to standard specimens and non-standard specimens in fracture toughness tests [22]. The aim of this work was studying the applicability of this methodology for *coiled tubing* specimens. Due to *coiled tubing* diameter and thickness, no standard specimens must be used. To overcome this problem, specimens were made with *coiled tubing* pieces. Because the specimens were not standard, the tests were carried out adapting Chattopadhyay et al. [23] tube tests to the *coiled tubing* dimensions. The evaluation of  $J$ -integral from test data was made by the derived limit load analyses developed by Chattopadhyay et al., based on expressions of  $\eta^{pl}$  and  $\gamma$  functions.

Test specimens consisted of coiled tubing segments, of 1 m long approximately. The geometry function was experimentally obtained from testing blunt notched *coiled tubing* specimens with different arc length to width,  $2C/W$ , ratios. Once the geometry function was determined, the  $S_{pb}$  method was used to estimate stable crack growth on a *coiled tubing* fracture mechanics test. The results were compared with those obtained by applying the potential drop method -used as reference method- and fracture surface measurements.

**2. Material and methods**

Test specimens were cut-out from two coiled tubing materials called A and B. They consisted of coiled tubing segments, of 1 m long approximately, with through wall circumferential cracks, machined by a milling machining process. Two crack

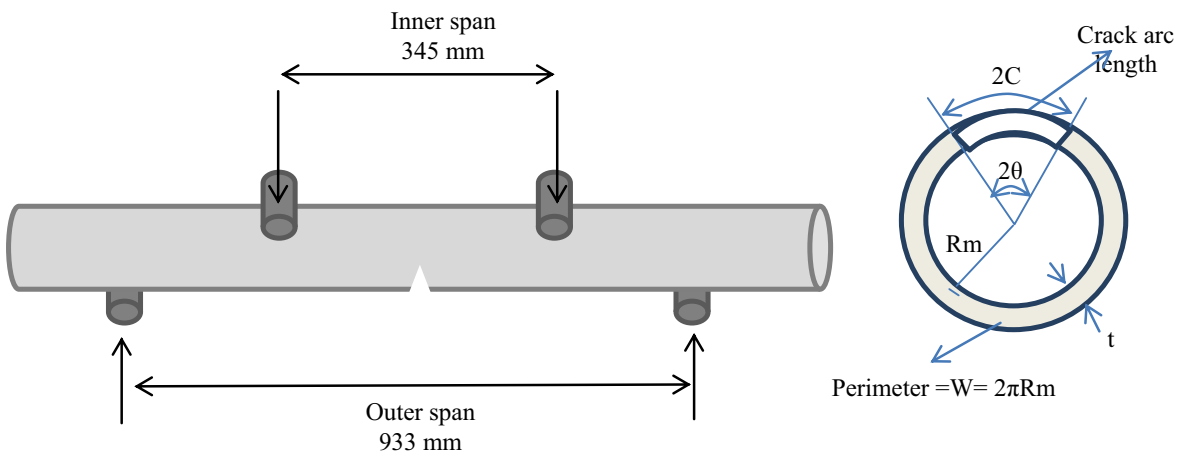


Fig. 1. Pipe with through wall circumferential crack under four-point bending load scheme.

front configurations were tested, precracked (PC) and blunt notched (BN) in order to apply  $S_{pb}$  method to estimate crack extension.

Four point bending loading was applied to all specimens in a Wolpert Universal Testing Machine at room temperature. An inner span of 345 mm and an outer span of 933 mm were applied, Fig. 1. Only the precracked specimens were fatigue precracked (2–10 mm at each side) before performing the fracture tests. This ensured a sharp crack tip. The geometric details of the tested specimens are given in Tables 1 and 2.

Load, load line displacement and crack mouth potential were recorded during the tests. The direct current potential drop (DCPD) method represents one of the possibilities to measure crack length during fracture mechanics testing. The DCPD method works based on the occurrence of an electrical potential drop,  $\Delta E$ , caused by a discontinuity in a specimen, like cracks, when a direct current of a sufficient value passes through the whole specimen cross-section. The disturbance magnitude is a function of crack arc size and length. Advantages and problems related to the application of DCPD method were discussed [24,25]. The method requires a calibration curve which relates crack arc length with the corresponding potential drop. This curve was determined testing several blunt notched coiled tubing specimens, with different stationary crack arc lengths. The potential drop was measured for every blunt notched specimen applying a 30A direct current, passing through the whole specimen cross-section through the wires connected to the specimen. Potential drop was measured on the sides of the crack arc length.

Once the potential drop calibration curve was determined, fracture tests of precracked and blunt notched specimens were conducted. Coiled tubing segment specimens were isolated with MICA plates (silicate mineral) between four point bending rollers and the tube segments.

**Table 1**  
Details of BN test specimens for G(a/W) determination and potential drop calibration.

Mat	Blunt notched				
	Spec.	Out diameter [mm]	Wall thickness [mm]	2C [mm]	W [mm]
A	CTABN1	51.1	5.30	91.0	160.5
	CTABN2	51.1	5.30	96.0	160.5
	CTABN3	51.1	5.30	77.5	160.5
	CTABN4	51.1	5.30	83.5	160.5

**Table 2**  
Details of BN and PC specimens used for  $S_{pb}$  method application.

Mat	Blunt notched					Pre cracked				
	Spec.	Out diameter [mm]	Wall thickness [mm]	2C [mm]	W [mm]	Spec.	Out diameter [mm]	Wall thickness [mm]	2C <sub>0</sub> [mm]	W [mm]
B	CTBBN12	51.1	5.30	102	160.5	CTBPC1	51.1	5.30	72.6	160.5
	CTBBN1	51.1	5.30	94.8	160.5	CTBPC2	51.1	5.30	72.2	160.5
	CTBBN2	51.1	5.30	76.0	160.5	CTBPC3	51.1	5.30	86.8	160.5

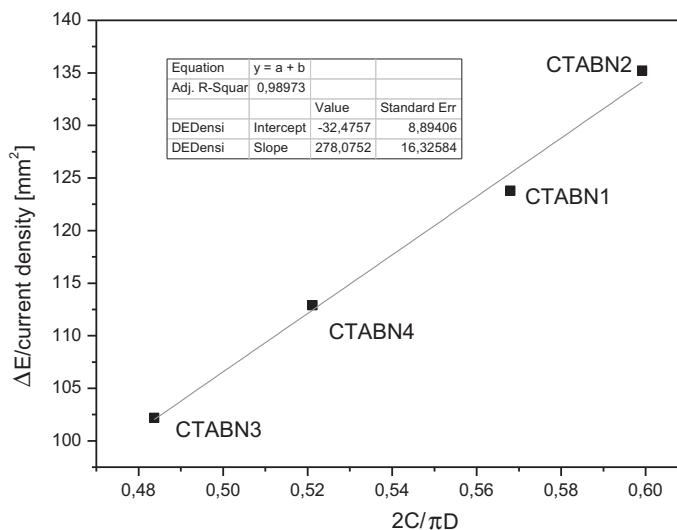


**Fig. 2.** Potential drop calibration curve.

After testing, specimens were heat tinted, then cooled and broken. The initial and final crack arc lengths were measured on the fracture surface.

### 3. Results and discussion

#### 3.1. Potential drop calibration

The potential drop calibration was performed testing different  $2C/W$  ratios on blunt notched coiled tubing specimens, where  $2C$  is the *coiled tubing* crack arc length, and  $W$  the tube perimeter used as width, Fig. 1. Calibration obtained is shown in Fig. 2. The potential drop measured was normalized with the current density in order to be independent of the coiled tubing diameter and thickness.

#### 3.2. Geometry function $G(a/W)$ determination

The blunt notched specimens described in Table 1 were tested up to maximum load in order to determine the geometry function  $G(2C/W)$  for coiled tubing, where  $2C$  is the *coiled tubing* crack arc length. Fig. 3 shows the load vs. plastic displacement records of material A.

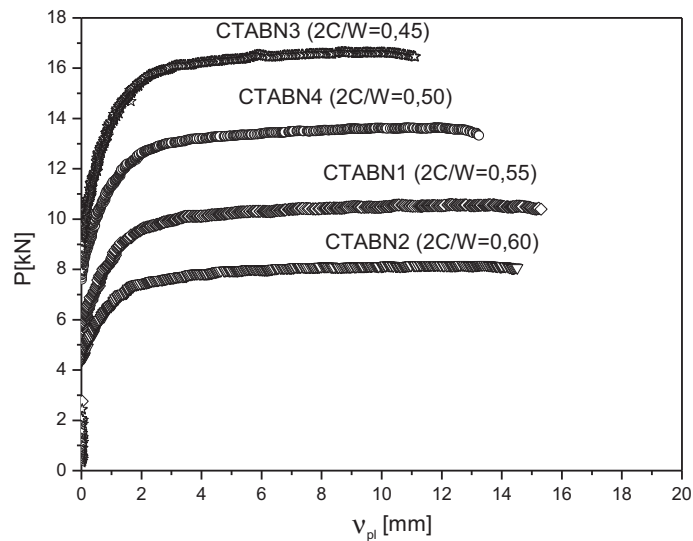


Fig. 3. Load vs plastic displacement of blunt notched specimens.

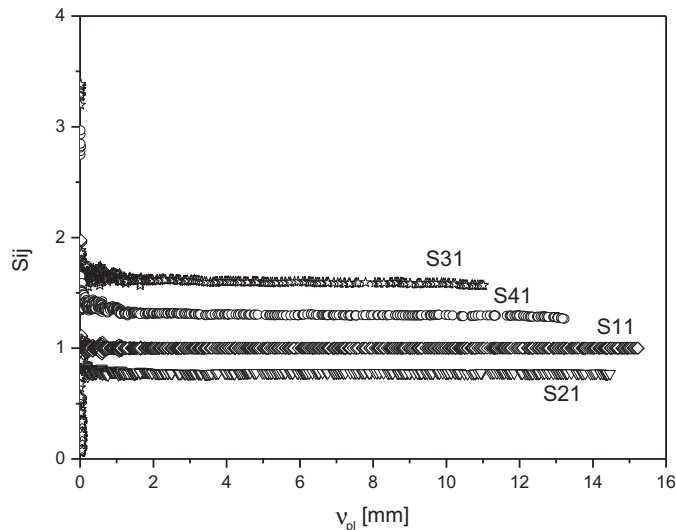


Fig. 4.  $S_{ij}$  parameter vs plastic displacement.

Fig. 4 shows the  $S_{ij}$  parameters calculated from the load ratio between two blunt notched specimens at constant displacement. The separability parameter is almost constant for the whole range of plastic displacement, except for a limited region at the beginning of plastic behavior. The  $S_{ij}$  parameter constancy evidence the existence of the separability property for this material and configuration for a wide range of crack lengths.

Fig. 5 shows the geometry function determined [26] fitting a potential function to the  $S_{ij}$  vs.  $b_0/W$  values. This allowed the use of the  $S_{pb}$  method for 4P bend coiled tubing testing.

### 3.3. The use of $S_{pb}$ method for coiled tubing specimens

Precracked and blunt notched coiled tubing specimens showed in Table 2 were tested. A testing scheme in four-point bending with potential drop implementation is shown in Fig. 6a–c show the fracture surfaces of precracked and blunt-notched specimens respectively.

Fig. 7 shows the load vs. plastic displacement obtained for both configurations and both materials.

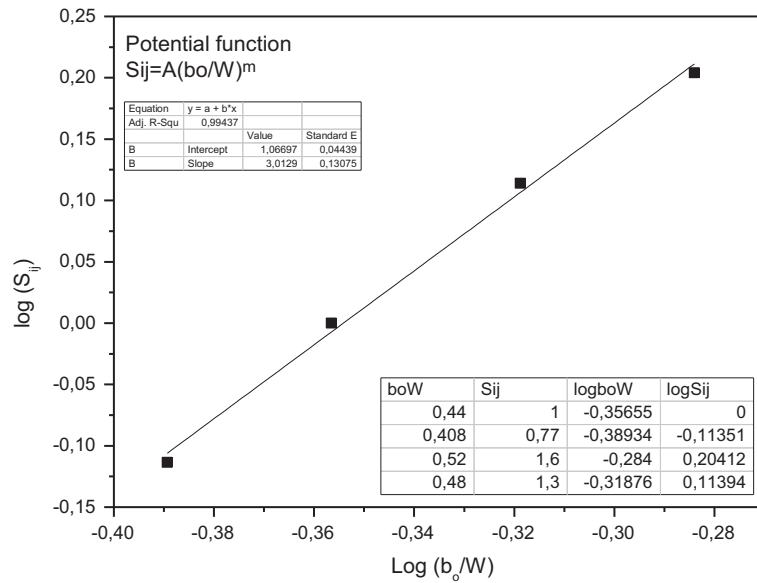


Fig. 5.  $S_{ij}$  vs.  $b_0/W$ .

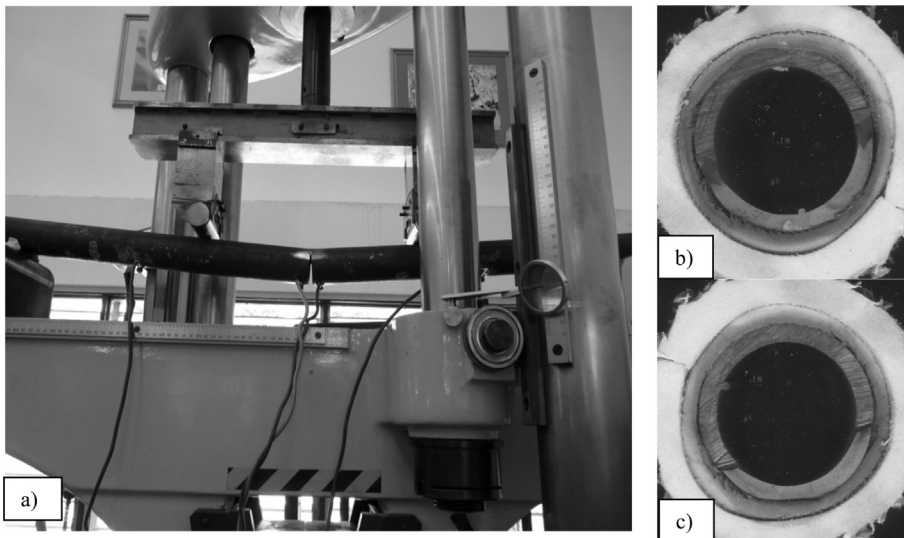


Fig. 6. (a) Precracked coiled tubing fracture test. (b) Precracked coiled tubing fracture surface. (c) Blunt notched coiled tubing fracture surface.

According to the  $S_{pb}$  method definition, it is required that the blunt notched specimens should have at least the same plastic displacement than the precracked specimens. Fig. 7 shows that none of the blunt notched specimens fulfill this require-

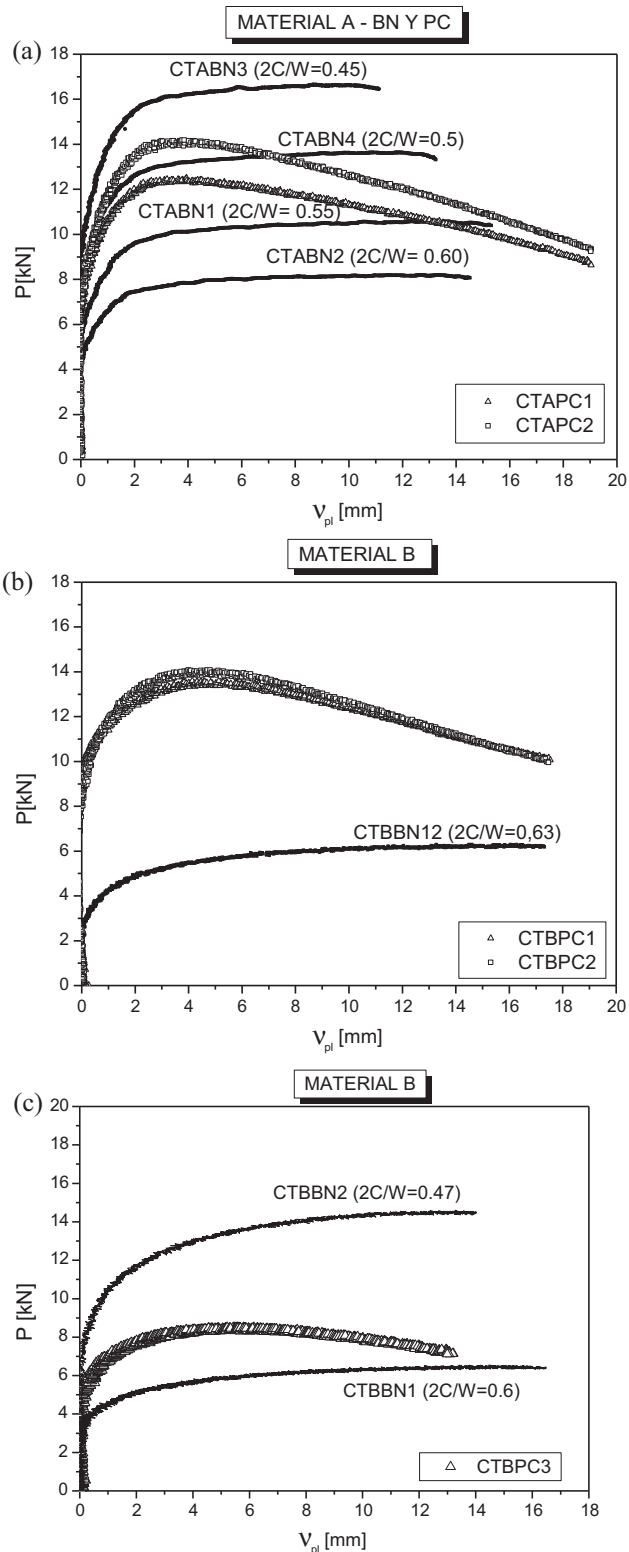


Fig. 7. Load vs plastic displacement for precracked and blunt notched coiled tubing specimens. (a) Material A, (b and c) Material B.

ment for Material A. Instead, for material B, CTBBN12 presented the same plastic displacement than the precracked specimens CTBPC1 and CTBPC2, and CTBBN1 and CTBBN2 presented more plastic displacement than the precracked specimen CTBPC3. Hence, the  $S_{pb}$  method was applied only to material B.

Blunt notched specimens Material A began to suffer an incipient crack growth and the tests had to be stopped at a lower plastic displacement than the already tested precracked specimens. This method limitation was already noted in a previous paper [27].

$S_{pb}$  parameter was determined as shown in Fig. 8.

Crack lengths for every point of the load vs. plastic displacement curves were determined by applying Eq. (5). It is important to note that in order to use  $S_{pb}$  method for *coiled tubing* specimens the geometry function had to be determined, as it was obtained in point 3.2 of this work. Besides, due to coiled tubing fracture specimens were *coiled tubing* segments, the letter  $a$ , which represents the crack length in a standard fracture toughness specimen, was changed to  $2C$  because in *coiled tubing* segment specimens the crack is a crack arc length, Fig. 1.

Fig. 9 shows crack arc lengths  $2C$  obtained by the  $S_{pb}$  method together with potential drop and fracture surface measurements.

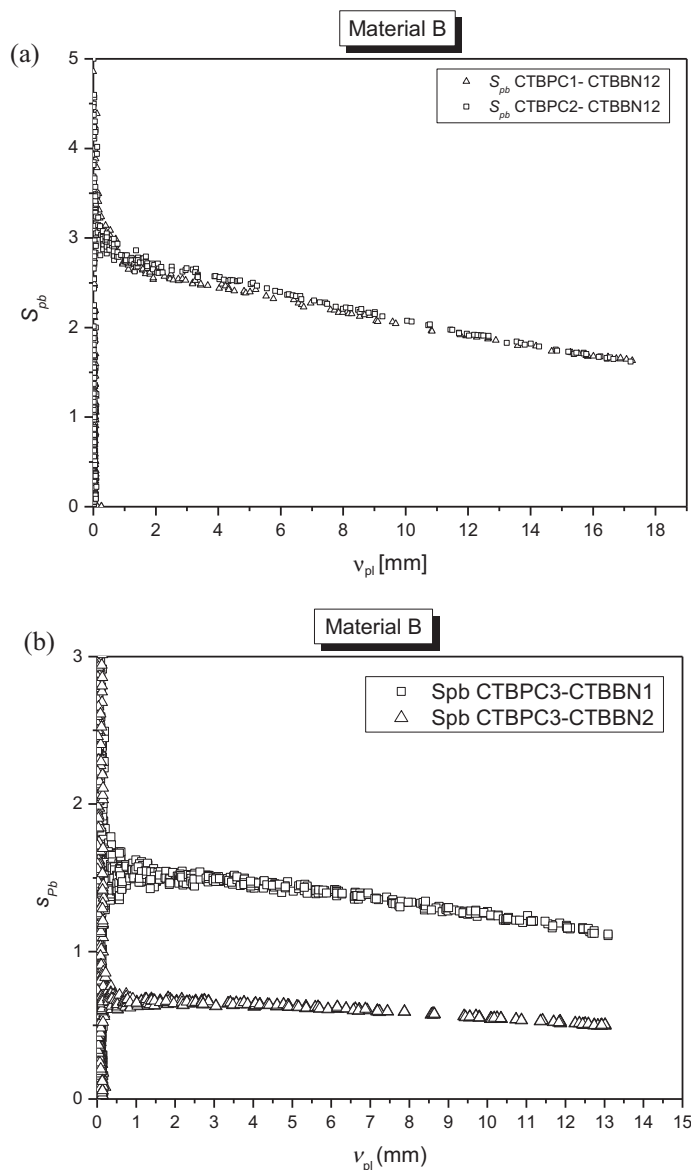


Fig. 8.  $S_{pb}$  parameter vs. plastic displacement.



Measurements on *coiled tubing* fracture surface for final crack arc lengths were not simple due to tunneling occurring on the crack front and roundness of the specimens after tested. Anyway nine measurements were made for each arc length and an average value was obtained. Fig. 10a.

$S_{pb}$  method estimates a lower initial crack length for specimen CTBPC2 of material B, being the highest difference 3.46%, Table 3, while PD underestimated the crack lengths in a 1.66%. On the other hand,  $S_{pb}$  presented a better behavior for material C, estimating initial crack lengths for both specimens with a difference with fracture surface of 1.95%.

The differences for final crack arc length were less than 1% for  $S_{pb}$  method and less of 5.34% for potential drop method, Table 4.

Table 5 shows the stable crack arc growth differences between  $S_{pb}$  and potential drop methods with fracture surface measurements. For both materials the worst behavior of  $S_{pb}$  method was for specimen CTBPC2, in coincidence with the worst estimation of PD.

Two different blunt notched specimens with different  $2C/W$  were used for the same precracked specimen, CTBPC3. No appreciable differences were found on the crack length estimations.

As it was already mentioned above, some out of roundness was detected on the tubes fracture surface after testing. Diameters D1 and D2 were measured, as Fig. 11 shows, before and after de tests. Results are shown in Table 6.

The most appreciable out of roundness was found on specimen CTBPC2, in coincidence with the poorest behavior of method's estimations (see Fig. 9b).

The differences in estimated initial and final crack lengths were in all the cases less than 5.35% when compared to the fracture surface measurements. Instead, differences were larger when compared to potential drop measurements; although the more important error can be attributed to PD measurement, may be due to resistivity changes due to plastic deformation.

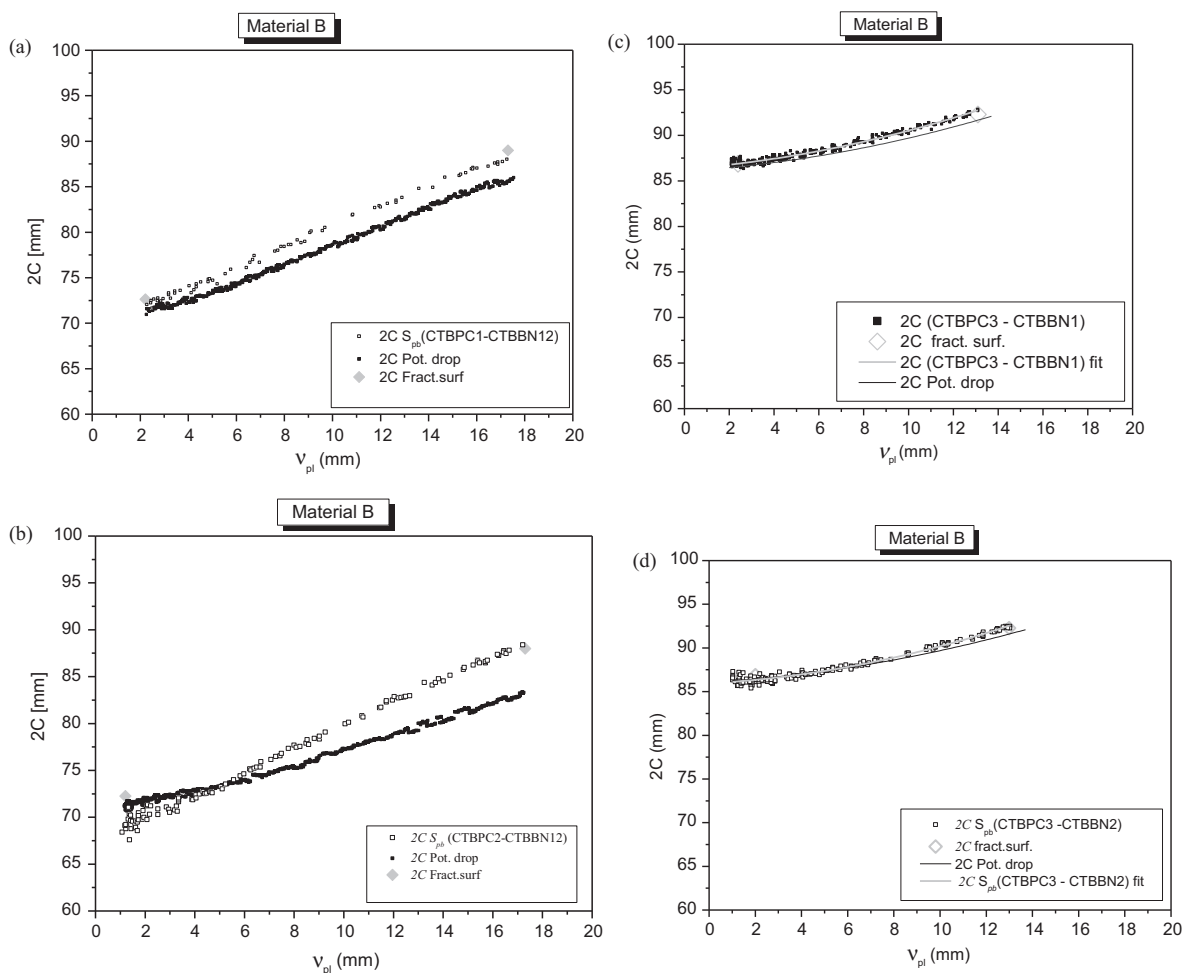


Fig. 9. Crack lengths obtained by  $S_{pb}$  method, potential drop and fracture surface measurements. (a) (CTBPC1- CTBBN12), Material B, (b) (CTBPC2-CTBBN12), Material B, (c) (CTBPC3 – CTBBN1), Material B, (d) (CTBPC3-CTBBN2), Material B.

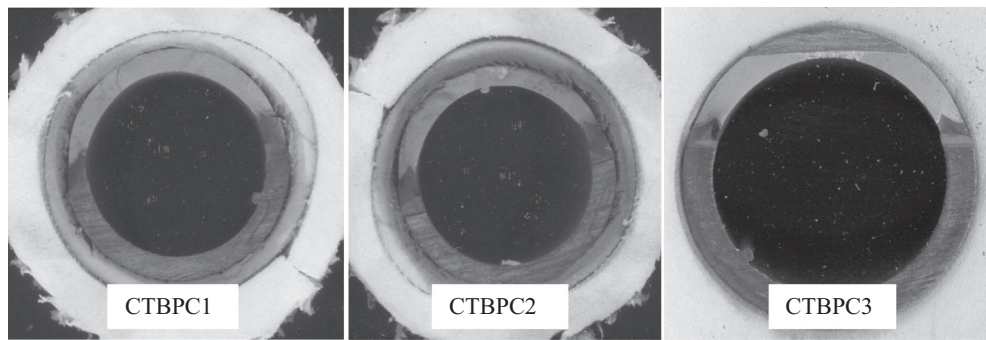


Fig. 10. Coiled tubings blunt notched fracture surface. Precracked coiled tubing specimens.

Table 3

Initial crack arc growth estimated by  $S_{pb}$  method, potential drop method and fracture surface measurements.

PC	BN	2Co Fract. Surf [mm]	2Co Pot. Drop [mm]	2Co $S_{pb}$ [mm]	% Diff. ( $S_{pb}$ -FS)	%Dif (PD-FS)
CTBPC1	CTBBN12	72.6	71.63	72.0	-0.82	-1.33
CTBPC2		72.2	71.0	69.7	-3.46	1.66
CTBPC3	CTBBN1	86.8	86.48	85.1	1.95	-0.13
	CTBBN2	86.8	86.48	86.2	-0.69	-0.13

Table 4

Final crack arc growth estimated by  $S_{pb}$  method, potential drop method and fracture surface measurements.

PC	BN	2Cf Fract. Surf [mm]	2Cf Pot. Drop [mm]	2Cf $S_{pb}$ [mm]	% Diff. ( $S_{pb}$ -FS)	%Dif (PD-FS)
CTBPC1	CTBBN12	88.9	85.9	88.0	-1.01	-3.37
CTBPC2		87.8	83.2	88.5	0.79	-5.34
CTBPC3	CTBBN1	92.3	91.7	92.3	0.00	0.65
	CTBBN2	92.3	91.7	92.6	0.32	0.65

Table 5

Stable crack arc growth estimated by  $S_{pb}$  method, potential drop method and fracture surface measurements.

PC	BN	$\Delta 2C$ Fract. Surf [mm]	$\Delta 2C$ Pot. Drop [mm]	$\Delta 2C$ $S_{pb}$ [mm]	% Diff. ( $S_{pb}$ -FS)	%Dif (PD-FS)
CTBPC1	CTBBN12	16.3	15.0	16.0	-1.84	-7.97
CTBPC2		15.6	12.4	18.8	20.5	-20.6
CTBPC3	CTBBN1	6.20	5.50	5.92	-4.51	-11.3
	CTBBN2	5.35	5.70	5.88	9.90	6.54

$JR$  curves were determined using  $S_{pb}$  and potential drop for crack length estimations. The  $J$ -integral evaluation from test data was made by using the derived limit load analyses developed by Chattopadhyay et al., based on expressions of  $\eta^{pl}$  and  $\gamma$  functions [23,28].

Due to differences in crack length estimations and  $\Delta 2C$  values obtained by  $S_{pb}$  and potential drop methods, the respective  $R$  curves do not coincide in all their extension. In every case, both curves present almost the same shape (see Fig. 12).

Fig. 13 shows all the  $JR$  curves determined by  $S_{pb}$  methodology. As it was reported in other authors work [28], coiled tubing  $JR$  curves varied with  $2C_0/W$ . Differences in initial slope could be related to in plane constraint dependence.

$S_{pb}$  method shows a good performance for crack length estimations and  $JR$  curves determination for coiled tubing non-standard specimens. Results are very encouraging. On the other hand, it seems to be a better performance of  $S_{pb}$  method when the extension of crack growth was lower than 7 mm, as in CTBPC3. No appreciable difference was observed in the  $S_{pb}$  method behavior due to different blunt notched crack length used.

Authors considered that more work ought to be done in applying  $S_{pb}$  method for tube specimens. The effect of roundness, amount of crack extension and crack tunneling could be further analyzed.

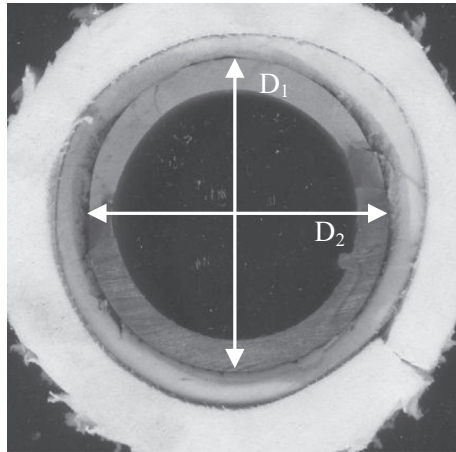


Fig. 11. Roundness measurement by diameters vertical and horizontal diameters  $D_1$  and  $D_2$ .

Table 6  
Roundness measurements.

PC	$D_{1i}$	$D_{2i}$	$D_{1f}$	$D_{2f}$	%Diff. $D_1$	%Diff. $D_2$
CTBPC1	51.02	50.99	51.15	50.73	+0.25	-0.51
CTBPC2	51.09	50.91	51.40	50.60	+0.60	-0.60
CTBPC3	51.15	50.70	51.28	50.65	+0.25	-0.10

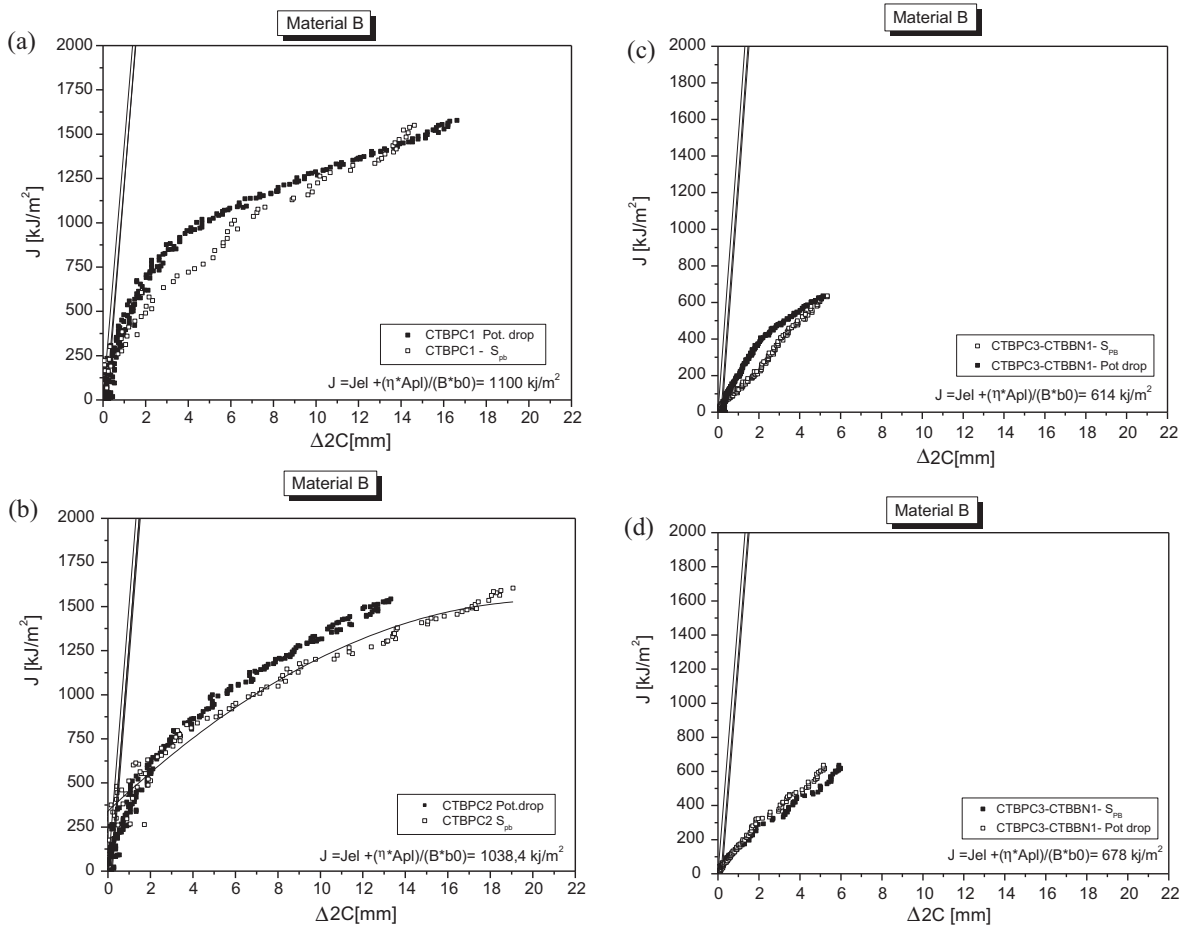


Fig. 12. JR curves for every coiled tubing specimen.

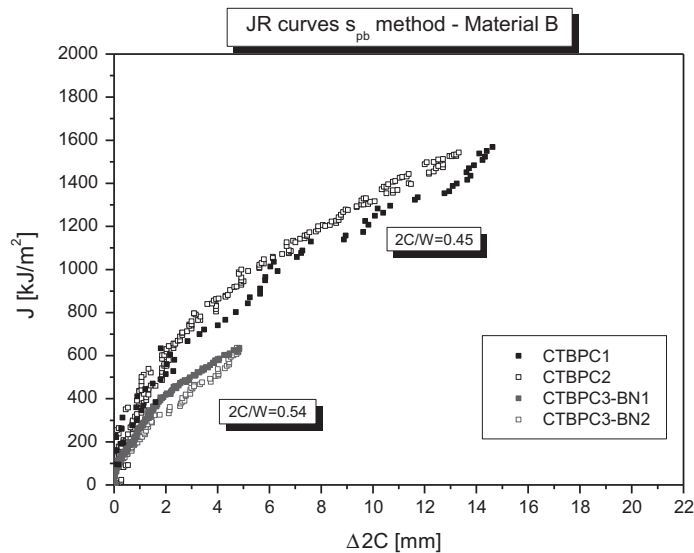


Fig. 13. Material B -  $J$ -R curves.

#### 4. Conclusions

Fracture toughness tests of *coiled tubing* are complex to be performed due to small thickness and diameter of the tubes. Non-standard specimens must be used. Considering these difficulties, in order to facilitate the task,  $S_{pb}$  method was applied to *coiled tubings* specimen configuration for the first time. It simplifies the crack length estimation without extra technology devices. For this purpose, geometry function was determined using blunt notched coiled tubing specimens for the applicability of the  $S_{pb}$  method on this kind of tubes.

Potential drop was also used as comparison and a calibration curve was also constructed.

The final crack length estimation differences of  $S_{pb}$  method and fracture surface measurements were lower than  $-5.34\%$ . In the case of total crack length extension the mayor difference was found on specimen that more out of roundness suffered.

$S_{pb}$  method shows a good performance for crack length estimations and  $J$ -R curves determination for coiled tubing non-standard specimens, simplifying times and facilities.

#### Acknowledgements

The authors want to acknowledge to Eduardo Benotti (GMF-UNComa) for his valuable collaboration. This work was supported by CONICET, and UNPSJB.

#### References

- [1] Tipton SM. Multiaxial plasticity and fatigue life prediction in coiled tubing. *Fatigue life time predictive techniques*. ASTM STP 1292 1996;3:283–304.
- [2] Rice JA. A path independent integral and the approximate analysis of strain concentration by notches and cracks. *J Appl Mech* 1968;35:379–86.
- [3] Begley JR, Landes JD. The  $J$  integral as a fracture criterion. In: Corten HT, Gallager JP, editors. *Fracture toughness ASTM STP 514*. West Conshohocken, PA: ASTM International; 1972. p. 1.
- [4] ASTM E1820-08: standard test method for measurement of fracture toughness, A.15 normalization data reduction technique. *Annual Book of ASTM Standards*, ASTM International, West Conshohocken, PA, 2008, p 10.
- [5] Bakker A. A DC potential drop procedure for crack initiation and R curve measurement during fracture ductile fracture test. In: Wessel ET, Loss FJ, editors. *Elastic-plastic fracture test methods: the user's experience*. ASTM STP 856. West Conshohocken, PA: ASTM International; 1985. p. 394.
- [6] Schwalbe KH, Hellman D, Heerens J, Knaack J, Muller-Ross J. Measurement of stable crack growth using the DC potential drop and the partial unloading methods. In: Wessel ET, Loss FJ, editors. *Elastic-plastic fracture test methods: the user's experience*. ASTM STP 856. West Conshohocken, PA: ASTM International; 1985. p. 338.
- [7] Herrera R, Landes JD. Direct  $J$ -R curve analysis: a guide to the methodology. In: Gudas JP, Joyce JA, Hackett EM, editors. *Proceedings of the fracture mechanics: twenty first symposium*, ASTM STP 1074. West Conshohocken, Philadelphia PA: ASTM International; 1990. p. 24.
- [8] Chung WN, Williams JG. Determination of JIC of polymers using the single specimen method. In: Joyce JA, editor. *Elastic plastic fracture test methods: the user's experience*. ASTM STP 1141. West Conshohocken, Philadelphia PA: ASTM International; 1991. p. 320.
- [9] Grellman W, Seidler S. *Engineering materials, deformation and fracture behavior of polymers*. Berlin: Editorial, Springer; 2001.
- [10] Cassanelli AN, Wainstein J, de Vedia LA. A study to estimate instantaneous crack length using the separability parameter  $S_{pb}$ . In: *Proceedings of ASME, applied mechanics and materials conference*. San Diego, California, USA: University of California; 2001. p. 27–9.
- [11] Wainstein J, de Vedia LA, Cassanelli AN. A study to estimate crack length using the separability parameter  $S_{pb}$  in steels. *Eng Fract Mech* 2003;70(17):2489–96.
- [12] Wainstein J, Frontini PM, Cassanelli AN.  $J$ -R curve determination using the load separation parameter  $S_{pb}$  method for ductile polymers. *Pol Test* 2004;23:591–8.

- [13] Bao C, Cai LX. Investigation on  $S_{pb}$  method based on nondimensional load separation principle for SEB and CT specimens. *Appl Mech Mater* 2004;117–119:480–8. doi: <http://dx.doi.org/10.4028/www.scientific.net/AMM.117-119.480>.
- [14] Bao C, Cai LX. Estimation of the  $J$ -resistance curve for Cr<sub>2</sub>Ni<sub>2</sub>MoV steel using the modified load separation parameter  $S_{pb}$  method. *J Zhejiang Univ – Sci A (Appl Phys Eng)* 2010;11(10):782–8. doi: <http://dx.doi.org/10.1631/jzus.A1000153>.
- [15] Likeb A, Gubeljak N, Matvienko YG. Finite element estimation of the plastic  $\eta_{pl}$  factors for pipe-ring notched bend specimen using the load separation method. *Fatigue Fract Eng Mater Struct* 2014;37(12):1319–29. doi: <http://dx.doi.org/10.1111/ffe.12173>.
- [16] Matvienko YG, Muravin EL. Numerical estimation of plastic  $J$ -integral by the load separation method for inclined cracks under tension. *Int J Fract* 2011;168(2):251–7. doi: <http://dx.doi.org/10.1007/s10704-010-9572-8>.
- [17] Wainstein J, Fasce LA, Cassanelli A, Frontini PM. High rate toughness of ductile polymers. *EngFractMech* 2007;74(13):2070–83.
- [18] Bernal CR, Cassanelli AN, Frontini PM. A simple method for  $J$ - $R$  curve determination in ABS polymers. *Pol Test* 1995;14:85–96.
- [19] Bernal C, Rink M, Frontini PM. Load separation principle in  $J$ - $R$  Curve determination of ductile polymers: a comparative analysis of the suitability of different materials deformation functions used in the normalization method. *Proceedings of Macromolecular Symposia* 1999;47(1):235–48.
- [20] Ernst HA, Paris PC, Landes JD. Estimation on  $J$  integral and tearing modulus  $T$  from single specimen record. In: Roberts R, editor. *Proceedings of the fracture mechanics: thirteenth conference ASTM STP 743*. West Conshohocken, PA: ASTM International; 1981. p. 476.
- [21] Sharobeam MH, Landes JD. The load separation and  $\eta_{pl}$  development in pre-cracked specimen test record. *Int J Fract* 1993;59:213–26.
- [22] Kim YS, Matvienko YG, Jeong HC. Development of experimental procedure based on the load separation method to measure the fracture toughness of Zr<sub>2.5</sub>Nb tubes. *Key Eng Mater* 2006;345–346:449–52. doi: <http://dx.doi.org/10.4028/www.scientific.net/KEM.345-346.449>.
- [23] Chattopadhyay J, Dutta BK, Kushwaha HS. Experimental and analytical study of three point bend specimen and through wall circumferentially cracked straight pipe. *Int J Pressure Vessel Piping* 2000;77:455–71.
- [24] Cerný I, Knei M, Linhart V. Measurement of crack length and profile in thick specimens and components using modified DCPD method. In: *Proceedings of the 5th int conf damage and fracturemechanics*, Bologna, June. Southampton, UK: Computational Mechanics Publications; 1998.
- [25] Cerný I. The use of DCPD method for measurement of growth of cracks in large components at normal and elevated temperatures. *Eng Fract Mech* 2004;71:837–48.
- [26] Sharobeam MH, Landes JD. The load separation criterion and methodology in ductile fracture mechanics. *Int J Fract* 1991;47:81–104.
- [27] Wainstein JE, Perez Ipiña JE. Load separation method  $S_{pb}$ , used to estimate crack extensions for JR curves modified for geometric variations in blunt notched remaining ligaments. *J Test Eval* 2017;45(4). doi: <http://dx.doi.org/10.1520/JTE20160027>. ISSN: 0090-3973.
- [28] Wainstein JE, Perez Ipiña JE. Fracture toughness of HSLA coiled tubing used in oil wells operations. *J Press Vessel Technol* 2011. doi: <http://dx.doi.org/10.1115/1.4004569>.